INIS-mf--6401

ZA8100086

SOME INTERESTING DEVELOPMENTS RELATING TO GAS DYNAMICS IN THE APPLICATION OF THE UCOR PROCESS FOR ISOTOPE SEPARATION

Presentation to

TWELFTH INTERNATIONAL SYMPOSIUM

on

RAREFIED GAS DYNAMICS

University of Virginia

July 7-11, 1980

T G Alant
W A Schumann

URANIUM ENRICHMENT CORPORATION OF SOUTH AFRICA LIMITED

VALINDABA

P O Box 4587
PRETORIA
0001
SOUTH AFRICA

Telephone 48-8111
Telex 30253

SOME INTERESTING DEVELOPMENTS RELATING TO GAS DYNAMICS IN THE APPLICATION OF THE UCOR PROCESS FOR ISOTOPE SEPARATION

Presentation to

TWELFTH INTERNATIONAL SYMPOSIUM

on

RAREFIED GAS DYNAMICS

University of Virginia

July 7-11, 1980

T.G. Alant

W.A. Schumann

URANIUM ENRICHMENT CORPORATION OF SOUTH AFRICA, LIMITED

Valindaba

P.O. Box 4587
PRETORIA
0001
SOUTH AFRICA

Telephone 488111

Telex 30253

SOME INTERESTING DEVELOPMENTS RELATING TO GAS DYNAMICS IN THE APPLICATION OF THE UCOR PROCESS FOR ISOTOPE SEPARATION

T G Alant and W A Schumann

Uranium Enrichment Corporation of South Africa, Ltd.

Valindaba

Republic of South Africa

INTRODUCTION

The South African uranium enrichment process is of an aerodynamic type and the separating element has been described as an advanced vortex tube [1]. Research and development in respect of the separating element was initiated in 1961 [2] and work during the first decade concentrated mainly on the improvement of this element. During the seventies the objective included the development of an enrichment process based on this element. This paper describes some interesting developments relating to gas dynamics in the application of the UCOR process for uranium enrichment [3;4].

CASCADE TECHNIQUE

The UCOR separating element has a very small cut, i.e. it has a high degree of asymmetry with respect to the UF_6 flow in the enriched and depleted streams, which emerge at different pressures. Conventional cascade arrangements are not very suitable for such elements, since they require a large number of elaborately connected stages to attain a high separative power efficiency.

Figure 1 shows a separating element with flow ratio μ; the symbol G designates mass flow of uranium hexafluoride (UF_6). The conventional cascade technique for an element with a small cut is illustrated in figure 2, which shows part of a cascade for an element with a UF_6 flow ratio μ of enriched to depleted streams equivalent to 1/3. The enriched stream from stage j goes to stage (j+3) and the depleted stream to stage (j-1). The enrichment factor between stages is 1/3 of the enrichment factor $\varepsilon_{\ell o}$ between the enriched and inlet streams of a stage. Figure 3 shows an alternative presentation of the same cascade arrangement. For the UCOR process the flow ratio μ is typically 0,045 to 0,055. For μ = 1/20 the cascade corresponding to that in figure 3 has 20 stages per group, with the enrichment factor between stages only 1/20 of $\varepsilon_{\ell o}$. The cascade can be simplified by recirculating part of the depleted stream of a stage to increase the effective cut, or by modifying the separating element. In both cases the separative efficiency is however markedly reduced.

In the helikon technique of cascading a large number of small stages are, in effect, incorporated in one module, and these stages share a common pair of axial compressors. The streams from different stages are introduced into a compressor in parallel, at different points on the inlet circumference, and are transmitted without excessive mixing between these streams. In our application each stream is divided into two and the component streams are then introduced symmetrically about a plane through the compressor axis, from segments formed by partitions in the radial direction, as illustrated in figure 4. In this way the concentration difference between adjacent streams is minimized. The partitions stop near the compressor inlet and commence again after the compressor outlet.

To simplify the presentation, we shall assume that a group of stages, as illustrated in figure 3, are all incorporated in a single module. The flow paths in such a module are schematically illustrated in figure 5. It is convenient to think in terms of a composition profile over the module rather than a stepwise change in composition, and to regard partitions simply as a means of maintaining the composition gradient, rather than as the boundaries of small stages. The deflection plates then do not transfer the flow from a given segment to the next segment, but rather cause the flow to swirl through the correct angle.

For the UCOR process the number of partitions for the depleted and feed streams are typically 2x20. In view of the small flow ratio μ, the separative power loss incurred by the mixing of adjacent enriched streams are relatively small and it can be shown that these streams can be handled by typically 2x5 segments per module, so that the intermodular piping is fairly simple.

MIXING IN AN AXIAL COMPRESSOR

The success of the helikon method is influenced by the amount of isotopic mixing losses in the axial flow compressors. We have found that the extent of gas mixing in an axial compressor can be predicted quite satisfactorily by a rather simple model based on the concept of a turbulent diffusivity.

According to Taylor [5, pp. 38-49] the mean-square displacement σ^2 of a fluid particle in time t may (for large values of t) be related to a diffusivity by an equation similar to that derived by Einstein for Brownian motion:

$$\frac{d\sigma^2}{dx} = \frac{2D_t}{U} ,$$

where the x-direction is the direction of flow, D_t is the eddy diffusivity and U the average velocity in the x direction over some period of time. If constant diffusivity is assumed, and $\sigma = \sigma_0$ when $x = x_0$, we get

$$(\sigma^2 - \sigma_0^2) = \frac{2 . D_t . (x - x_0)}{U} \qquad (1)$$

The problem of determining turbulent diffusivity is related to the problem of determining the turbulent Schmidt number, defined as

$$S_{ct} = \frac{\varepsilon}{D_t}$$

where

ε = effective (or virtual) kinematic viscosity.

If, according to Prandtl's theory, momentum and energy are transferred by the same mechanism in turbulent flow, it follows that S_{ct} = 1,0 and

$$D_t = \varepsilon \qquad (2)$$

Prandtl established a very simple equation for the apparent kinematic viscosity ε [6,p.550]. It is valid only in the case of free turbulent flow and was derived from extensive experimental data. In setting up his hypothesis, Prandtl assumed that the dimensions of the lumps of fluid which move in a transverse direction during turbulent mixing are of the same order of magnitude as the width of the mixing zone. The virtual kinematic viscosity, ε, is now formed by multiplying the maximum difference in the time-mean flow velocity with a length which is assumed to be proportional to the width, b, of the mixing zone. Thus,

$$\varepsilon = K.b.\ (U_{max} - U_{min})\ . \qquad (3)$$

Here K denotes a dimensionless number to be determined experimentally.

Substituting the local mean velocity U for the velocity difference in equation (3), and combining the above equations, it follows that

$$(\sigma^2-\sigma_o^2) = 2\ K.b.(x-x_o)\ .$$

In our application we are interested in the circumferential dispersion of the process gas at some mean radius $\bar{r}$. If σ_θ is the angle (in degrees) subtended by an arc of length σ at the radius $\bar{r}$, we have

$$\sigma = r.\ \frac{\sigma_\theta}{57,3}\ .$$

Taking X as the length of the compressor and interpreting b as the blade pitch s, the "mixing angle" or "standard deviation" σ_θ introduced by the compressor can be expressed as

$$\sigma_\theta \cong \left(\frac{81,0}{\bar{r}}\right).\ (K.s.X)^{\frac{1}{2}}\ .$$

According to this equation, short compressors with a large diameter and a small blade pitch introduce the least mixing. An approximate value for the Prandtl constant K is 1/50 for a good design.

It is of course clear that several rather complicated mechanisms contribute to mixing in a compressor. Experimental results show that blade loading is an important factor: for a compressor at constant speed, mixing increases when the operating point shifts towards the surge line. This is illustrated in figure 6.

As illustrated in figure 7, more mixing occurs at the annulus walls than at the average radius $\overline{r}$; therefore mixing may decrease as blade length increases, provided the swirl angle of the gas through the compressor does not vary radially.

The swirl angle should not vary radially since this introduces additional mixing as a result of radial diffusivity. A compressor with a blade design for a degree of reaction equal to unity fulfills this requirement beautifully.

RUN-UP OF THE COMPRESSORS

The separating element not only causes isotope separation, but also a degree of "gas separation", i.e. separation between the process gas (UF_6; mean molecular mass approximately 352 g/mole) and the carrier gas (H_2; molecular mass approximately 2,0 g/mole). Equilibrium operating conditions of the separating element in terms of mean molecular mass (M), volume flow (Q) and pressure (p) are shown on figure 8 for a module in total reflux.

Before start-up, the module is filled with a gas mixture of mean molecular mass $\overline{M}$ at the mean pressure $\overline{p}$, where

$$M_\ell < \overline{M} < M_o < M_s \quad \text{and} \quad p_\ell < p_s \cong \overline{p} < p_o \ .$$

The subscripts o, ℓ and s refer to the inlet, enriched and depleted streams of the separating element, respectively.

Interesting phenomena occur during the run-up of the compressors. Where the enriched (or light) stream compressor handles gas with a mean molecular mass of M_ℓ at essentially pressure p_ℓ at its design point, it handles gas of mean molecular mass $\overline{M}$ at pressure $\overline{p}$ when started. During the short run-up period the density of the inlet gas thus changes by a factor of something like 2; the corresponding factor is relatively small for the inlet stream compressor.

During the acceleration period pressure drops develop over the separating element. Eventually the element starts separating, causing the mean molecular mass of the "light" stream leaving the element to decrease. Since there is a finite channel volume between the separating element and the compressor, there is a time lag before lighter gas reaches the light stream compressor. The form of such a mean molecular mass (or density) front and the speed at which it moves through the system is determined by the run-up times of the compressors. These fronts may give rise to rapid changes in pressure rise across and mass flow through the light stream compressor, with the possibility of surge at a relatively high compressor speed.

Another interesting point concerns the run-up times of the compressors. The light stream compressor handles a relatively light gas and must deliver a relatively high pressure rise, compared to the inlet stream compressor. The nett result is that the operating speed of the light stream compressor is 2 to 3 times that of the inlet stream compressor. Since the aerodynamic load on a compressor only becomes important near full speed, the run-up times are mainly determined by the effective moments of inertia and the torque-slip curves of the motors. With normal motor designs, the typical run-up time of the light stream compressor can therefore be expected to be substantially longer than that of the inlet stream compressor. However, if the inlet stream motor runs substantially faster than the enriched stream motor, the flow of the enriched stream leaving the separating element may be too small for the enriched stream compressor and its working point may move towards the surge limit.

A further point to keep in mind is that the run-up times of the compressors must be relatively short to ensure quick passes through the critical speeds. On the other hand, if the run-up time is very short, the speed of the light stream compressor will be rather high when the front of "lighter" gas reaches it, with the possibility of surge.

In simulating the run-up of the compressors, we made the assumption that a compressor adapts itself to a change in working conditions immediately, i.e. that at any moment during the transient run-up period the compressor performance can be deduced from the performance map which applies to stationary conditions. Incidentally, this assumption is satisfactorily valid for our separating element.

After intensive studies, we arrived at the following general conclusions:

(a) With the gas inventory within reasonable limits, the inlet stream compressor may be run on its own.

(b) Under certain conditions regarding the gas inventory of the module, for example when the module is loaded with hydrogen only, the light stream compressor may be run on its own.

(c) With the gas inventory within certain limits, the compressors may be run up simultaneously. Expressing compressor speed as a percentage of full speed, there are certain limits on the allowable speed difference between the compressors during run-up, and the run-up time must not be too short. This implies limits on the torque-slip curves of the motors; we have found that these requirements can be easily met.

In figure 9 some of the interesting run-up characteristics relating to the enriched stream compressor are shown for a case of simultaneous run-up of the compressors.

AN INTERESTING HYDROSTATIC PHENOMENON

Gas separation not only causes interesting transients during run-up, but is also responsible for some noteworthy hydrostatic features of the system.

In practice various leak and diffusion possibilities exist between adjacent flow channels in a module. Because of the complexity of the system of compressors, separating elements, and interconnected channels with various possibilities of flow mixing and diffusion phenomena occurring between them, we consider a very simple and special case to demonstrate that under certain conditions spontaneous pressure and concentration gradients may arise.

Consider a helikon module in full reflux. Imagine each of the axial compressors to consist of a number of small parallel compressors. With reference to figure 10, the two parallel systems A and B of compressors and separating elements represent two adjacent channels in a helikon module.

For illustrative purposes, we consider a hypothetical case where only the following leakpath possibilities exist:

(i) Between waste stream channels upstream of the mixing point of the enriched and depleted streams, i.e. between points 1 and 2.

(ii) Between feed stream channels, i.e. between points 3 and 4.

It is further assumed that no mixing occurs in the compressor.

If the gas inventories of the two systems were the same, the operating conditions would be identical and no pressure differentials would exist to cause any leaks. In particular, the condition

$$M_{oA} = M_{oB} \tag{5}$$

would be satisfied. On the other hand, suppose a small disturbance in the inventories of the systems, such that

$$M_{oA} > M_{oB} .$$

In this case, due to the characteristics of axial compressors and the separating element, operating conditions in the two systems will drift towards the solution

$$M_{oA} = M_{sB} > M_{oB} , \tag{6}$$

with leaks occurring between points 1 and 2, and 3 and 4, respectively, since

$$p_{oA} > p_{oB} \quad \text{and} \quad p_{sB} > p_{sA} .$$

It can be shown that solution (6) represents the stable state.

The operating characteristics of axial compressors and of the separating element thus produce a driving force which tends to cause mole mass and associated pressure gradients to occur circumferencially in a helikon module. However, our module design provides enough equalising driving forces due to other leaks paths, and especially due to compressor mixing, to cancel the above effect for all practical purposes.

ACKNOWLEDGEMENTS

We are indebted to several colleagues who have contributed to the above work. The Board of Directors of UCOR are thanked for permission to publish this paper.

REFERENCES

[1] Roux, A.J.A., Grant, W.L., Barbour, R.A., Loubser, R.S., and Wannenburg, J.J., "Development and Progress of the South African Enrichment Project", Paper IAEA-CN-36/300 (II.3) presented at the International Conference on Nuclear Power and its Fuel Cycle, Salzburg, Austria, 2-13 May, 1977.

[2] Roux, A.J.A. and Grant, W.L., "Uranium Enrichment in South Africa", *Nuclear Energy Maturity, Proceedings of the European Nuclear Conference,* Paris, 21-25 April, 1975, Invited Sessions, pp. 167-171.

[3] Grant, W.L., Wannenburg, J.J., and Haarhoff, P.C., "The Cascade Technique for the South African Enrichment Process", in Papers on Developments in Uranium Enrichment presented at the 69th annual meeting of the American Institute of Chemical Engineers, Chicago, December 1 and 2, 1976, pp. 45-63.

[4] Haarhoff, P.C., *Tydskrif vir Natuurwetenskappe,* 16, Nr. 3 & 4, Sept. - Dec. 1976, pp. 68-126; trans.: "The Helikon Technique for Isotope Enrichment", Uranium Enrichment Corporation of South Africa (Ltd), report VAL-1, Nov. 1976.

[5] Sherwood, Thomas K. and Pigford, Robert L., *Absorption and Extraction,* McGraw-Hill Book Company, 1952.

[6] Schli hting, Hermann, "Boundary-layer Theory", 6th Ed., McGraw-Hill Book Company, 1968.

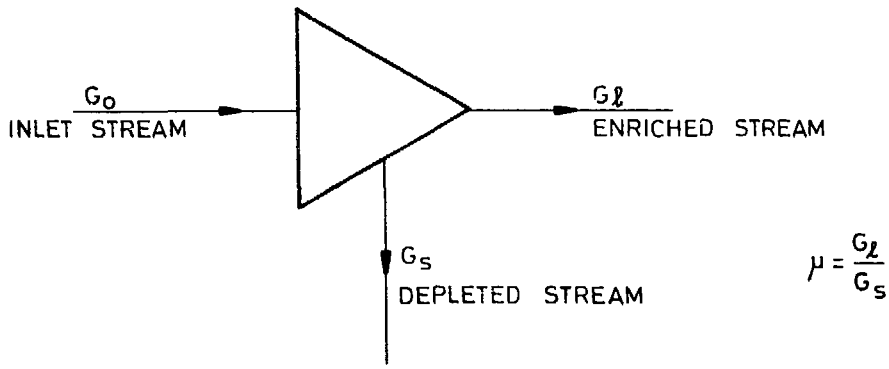

FIGURE 1: SCHEMATIC REPRESENTATION OF A SEPARATING ELEMENT WITH FLOW RATIO μ

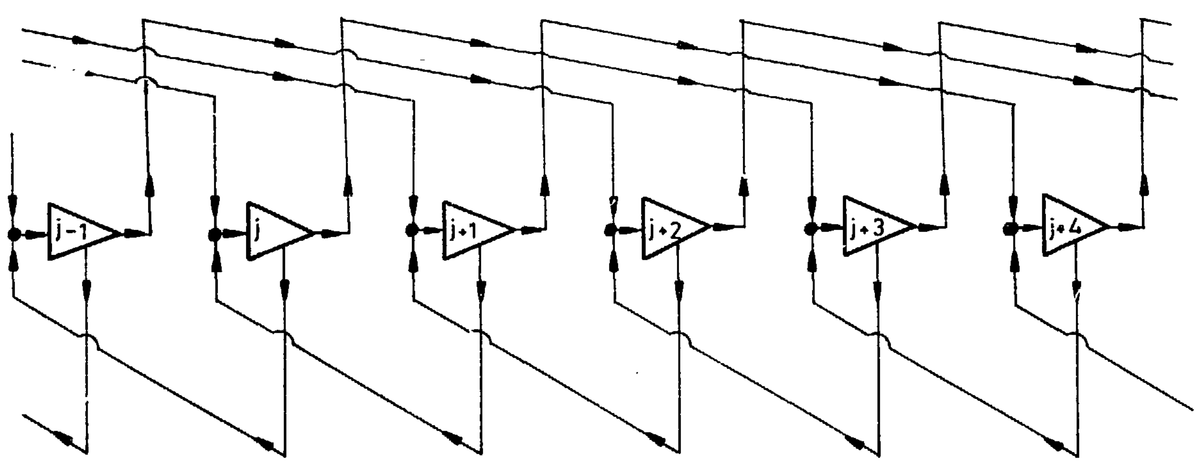

FIGURE 2: ARRANGEMENT OF SEPARATING ELEMENTS WITH $\mu = 1/3$ IN A COUNTERCURRENT CASCADE.

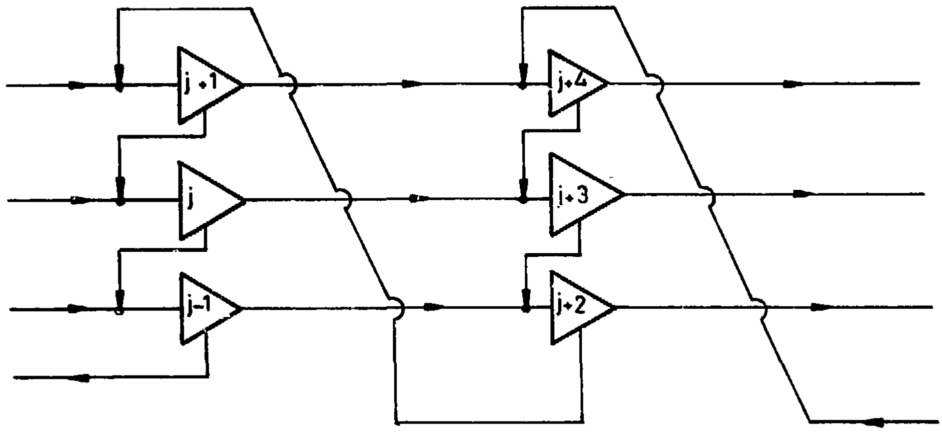

FIGURE 3: ALTERNATIVE PRESENTATION OF SEPARATING ELEMENTS WITH $\mu = 1/3$ IN A COUNTERCURRENT CASCADE

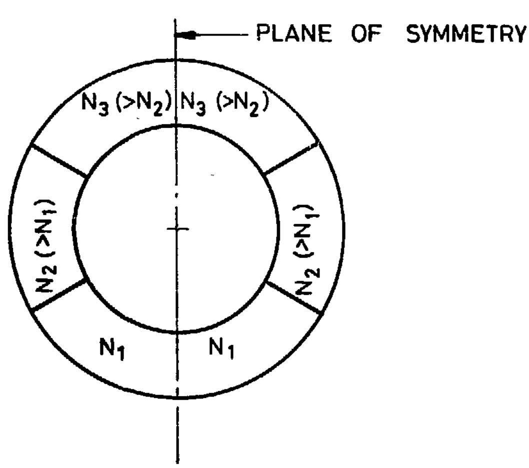

FIGURE 4: INTRODUCTION OF THREE STREAMS OF DIFFERENT $^{235}UF_6$ MASS FRACTIONS N_1, N_2 AND N_3 INTO A COMPRESSOR.

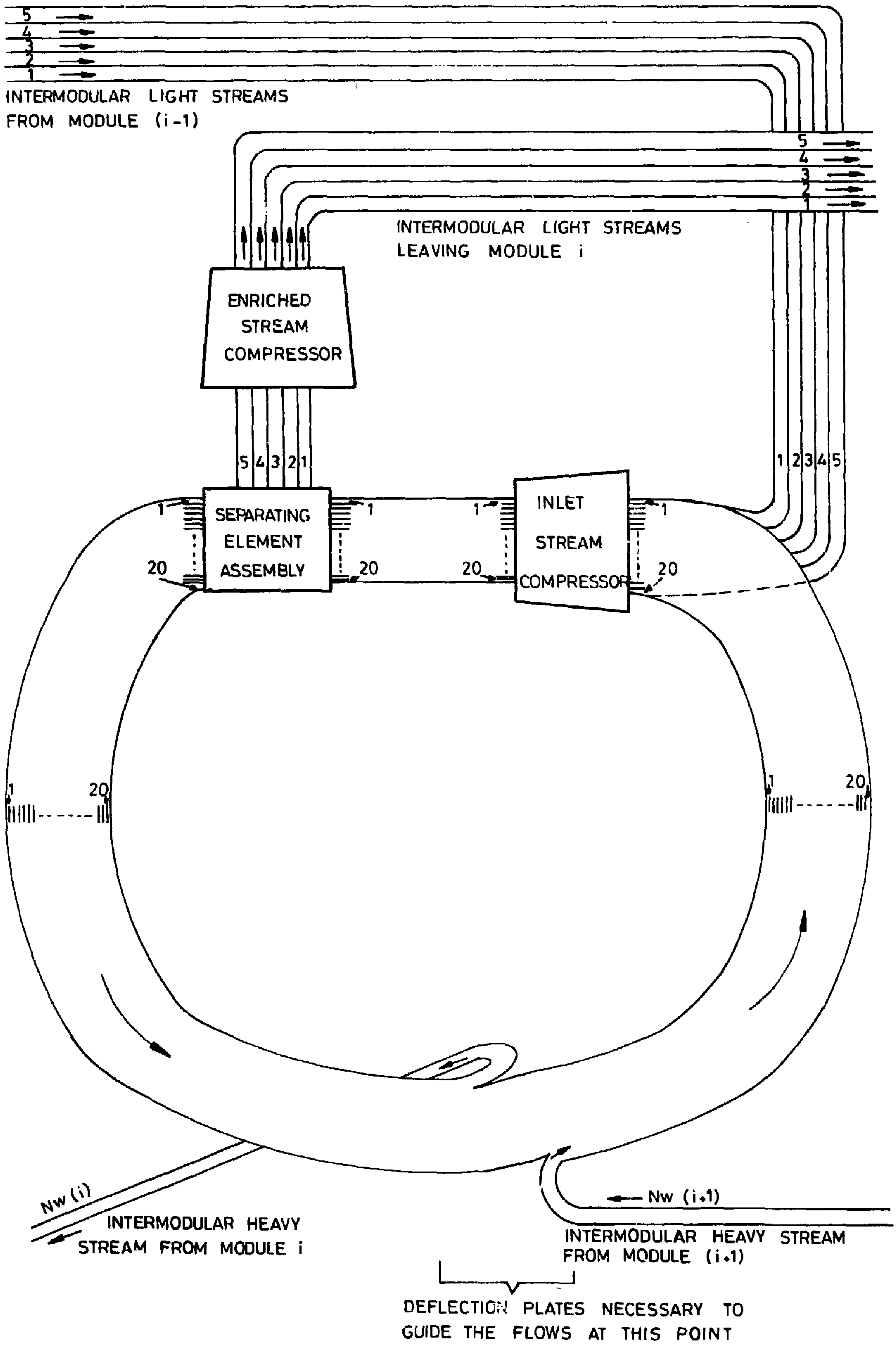

FIGURE 5: SCHEMATIC DIAGRAM OF MODULE i.

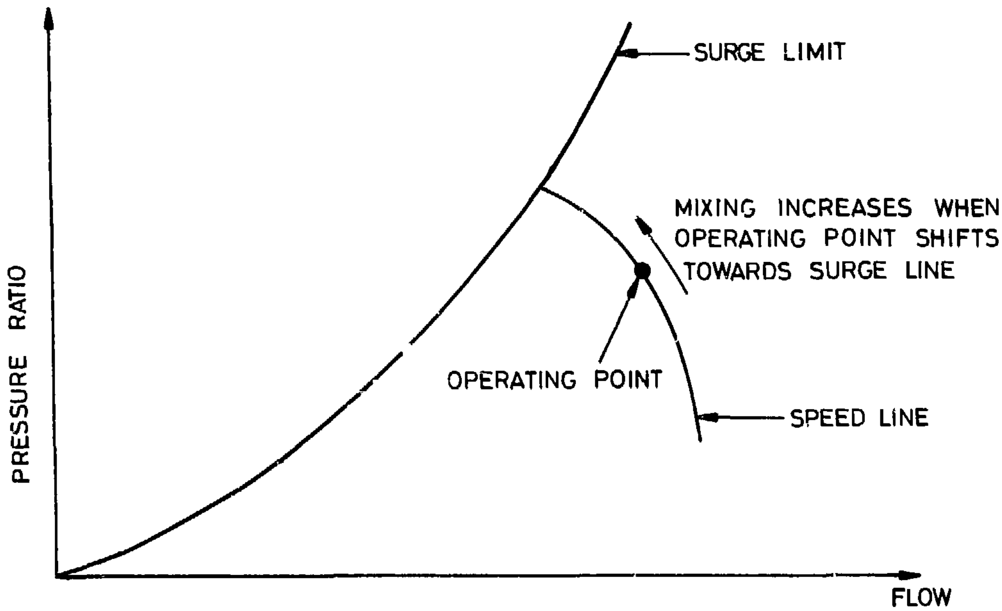

FIGURE 6: COMPRESSOR PERFORMANCE MAP ILLUSTRATING THE EFFECT OF BLADE LOAD ON MIXING IN THE COMPRESSOR.

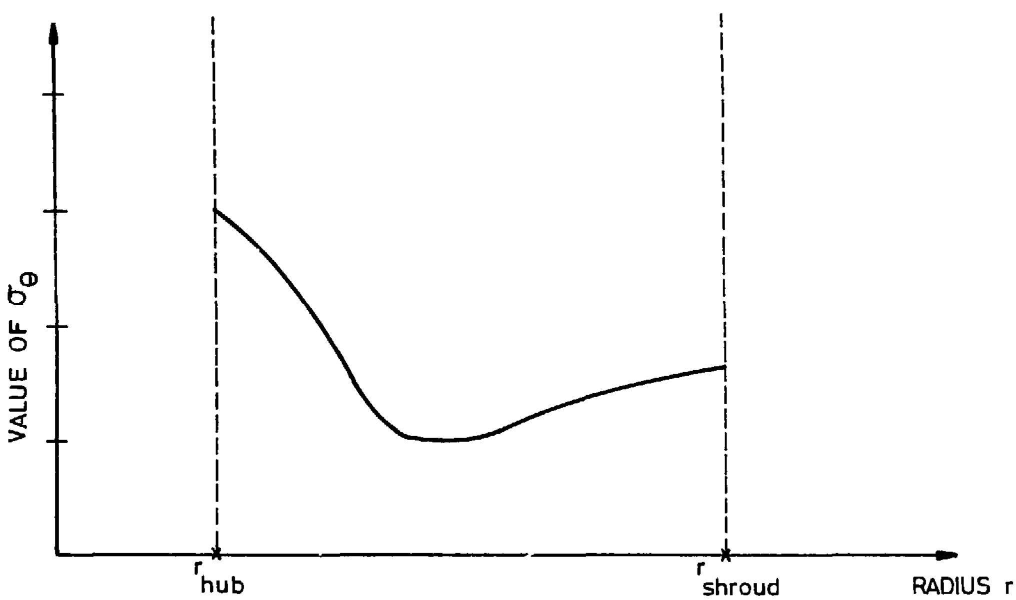

FIGURE 7: DIAGRAM ILLUSTRATING THE RELATIVELY INTENSE MIXING OCCURING NEAR THE ANNULUS WALLS IN AN AXIAL COMPRESSOR.

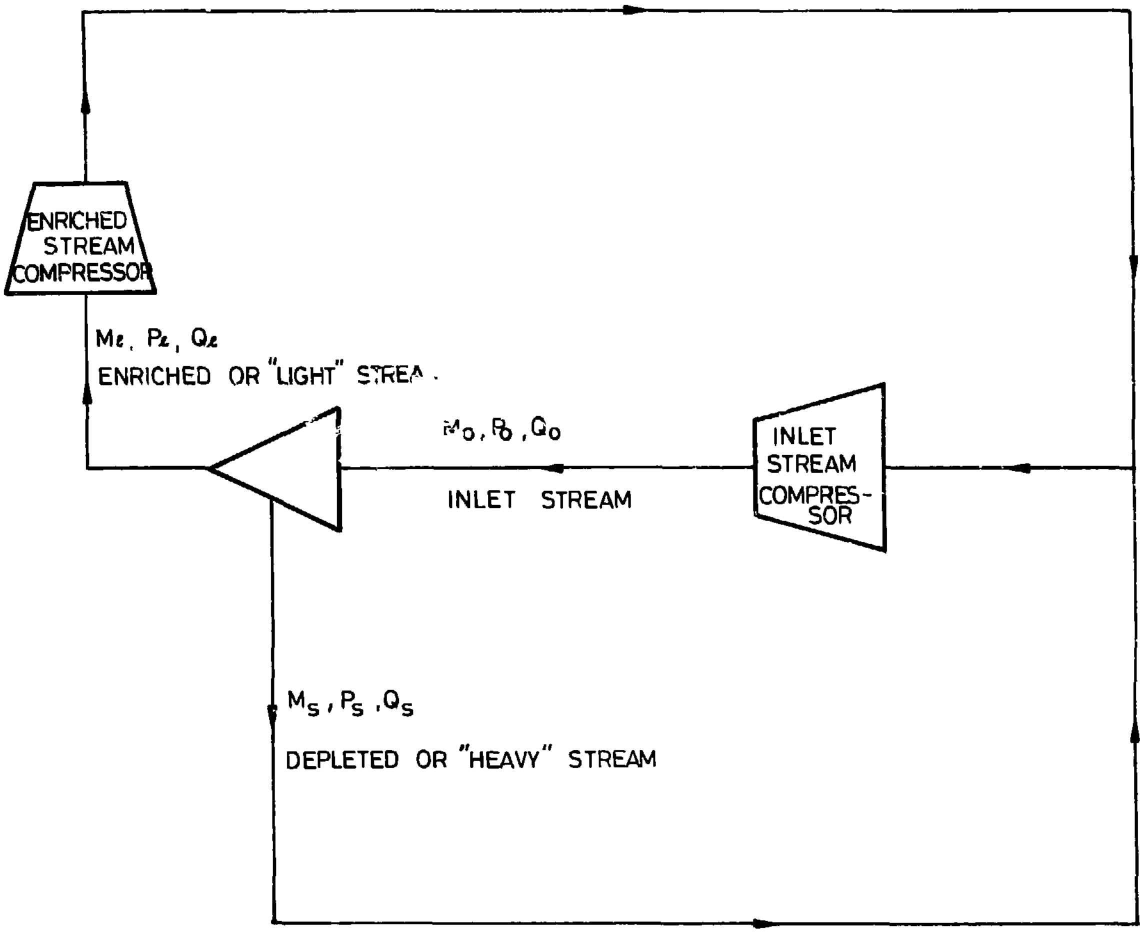

FIGURE 8: SCHEMATIC DIAGRAM OF A MODULE IN TOTAL REFLUX, WITH OPERATING PARAMETERS AROUND THE SEPARATING ELEMENT.

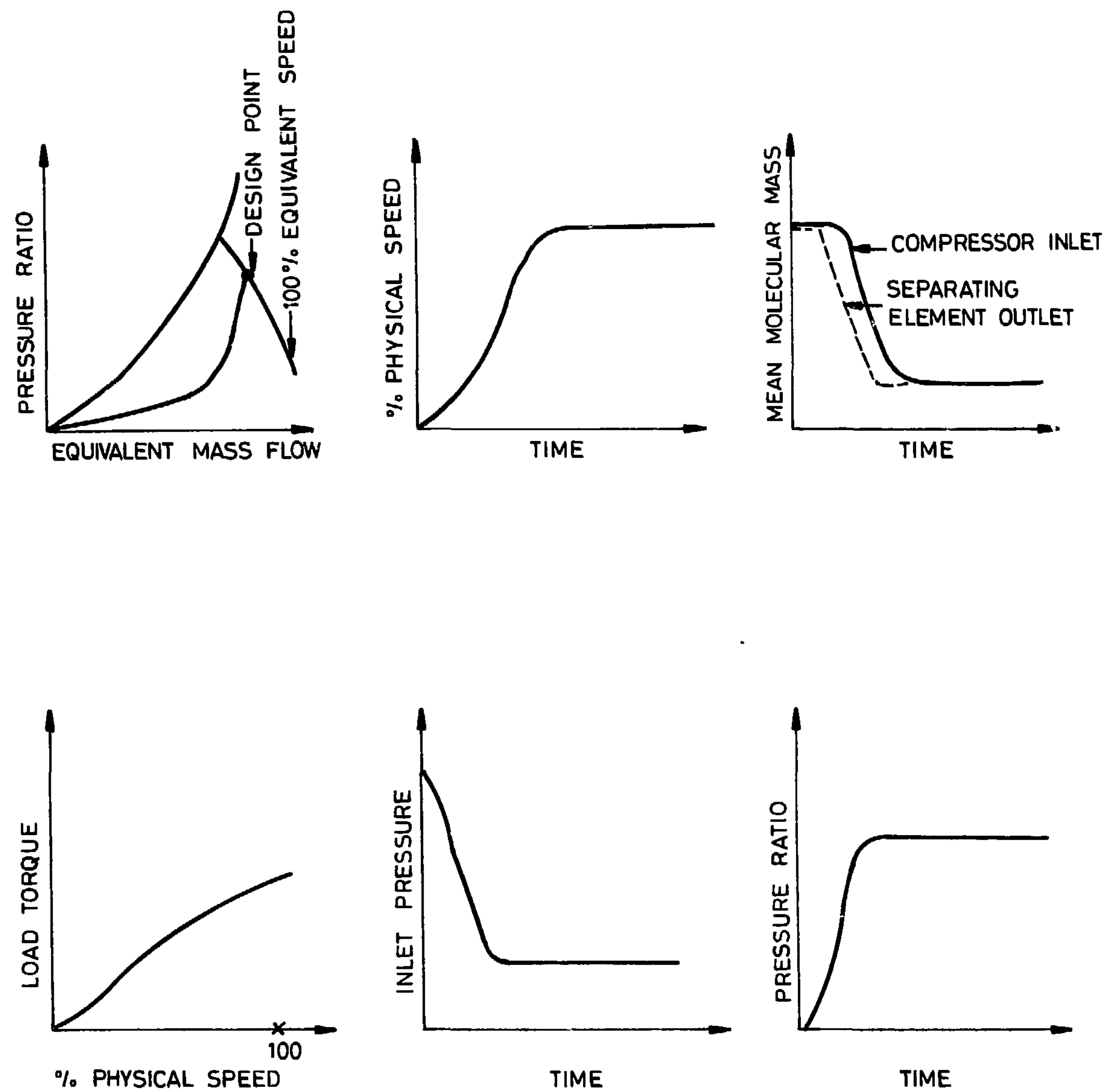

FIGURE 9: RUN-UP CHARACTERISTICS OF THE ENRICHED STREAM COMPRESSOR FOR A CASE OF SIMULTANEOUS RUN-UP OF THE COMPRESSORS.

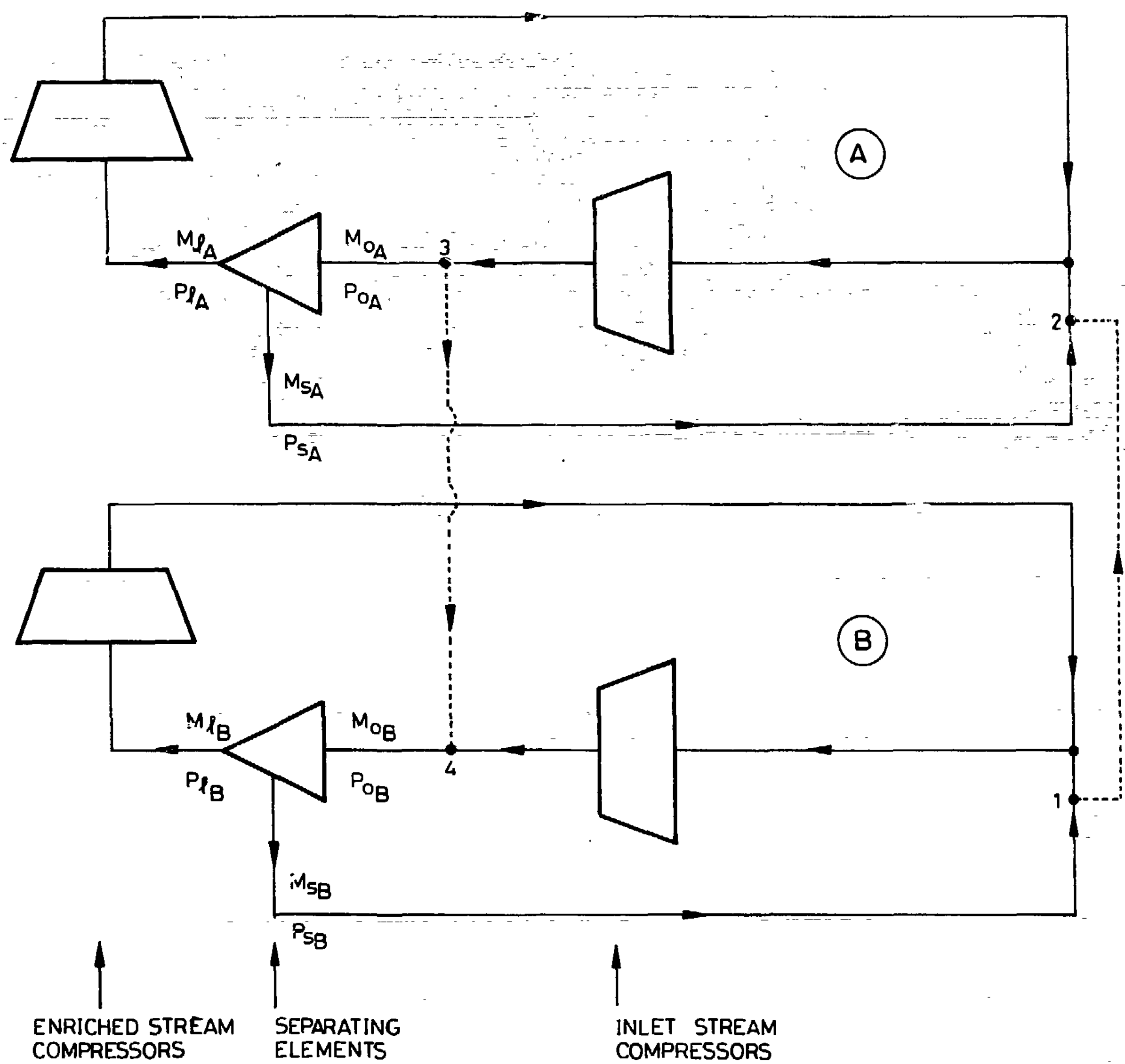

FIGURE 10 SCHEMATIC REPRESENTATION OF LEAKPATHS BETWEEN TWO PARALLEL SEGMENTS OF A HELIKON MODULE IN FULL REFLUX.